PHILOSOPHICAL TRANSACTIONS A

Research

CrossMark
click for updates

Author for correspondence:
Horacio M. Pastawski
e-mail: horacio@famaf.unc.edu.ar

Loschmidt echo in many-spin systems: contrasting time scales of local and global measurements

Pablo R. Zangara, Denise Bendersky,

Patricia R. Levstein and Horacio M. Pastawski

Instituto de Física Enrique Gaviola (CONICET-UNC), and Facultad de Matemática, Astronomía y Física, Universidad Nacional de Córdoba, Córdoba 5000, Argentina

(ID) PRZ, 0000-0001-7046-1345

A local excitation in a quantum many-spin system evolves deterministically. A time-reversal procedure, involving the inversion of the signs of every energy and interaction, should produce the excitation revival. This idea, experimentally coined in nuclear magnetic resonance, embodies the concept of the Loschmidt echo (LE). While such an implementation involves a single spin autocorrelation $M_{1,1}$, i.e. a local LE, theoretical efforts have focused on the study of the recovery probability of a complete many-body state, referred to here as global or many-body LE M_{MB}. Here, we analyse the relation between these magnitudes, with regard to their characteristic time scales and their dependence on the number of spins N. We show that the global LE can be understood, to some extent, as the simultaneous occurrence of N independent local LEs, i.e. $M_{MB} \sim (M_{1,1})^{N/4}$. This extensive hypothesis is exact for very short times and confirmed numerically beyond such a regime. Furthermore, we discuss a general picture of the decay of $M_{1,1}$ as a consequence of the interplay between the time scale that characterizes the reversible interactions (T_2) and that of the perturbation (τ_Σ). Our analysis suggests that the short-time decay, characterized by the time scale τ_Σ, is greatly enhanced by the complex processes that occur beyond T_2. This would ultimately lead to the experimentally observed T_3, which was found to be roughly independent of τ_Σ but closely tied to T_2.

THE ROYAL SOCIETY
PUBLISHING

1. Introduction

If an ink drop falls into a pond, the stain diffuses away until no trace of it remains whatsoever. One may naturally say that such a process is in fact irreversible. In the microscopic world, similar phenomena are also ubiquitous. For instance, let us consider a many-spin quantum system in thermal equilibrium where a local polarization excess is injected. Then, this excitation would spread all over as a consequence of spin–spin interactions. Such an apparently irreversible process is known as *spin diffusion* [1,2] and it can lead the system back to equilibrium. However, this naive picture has its limitations. On the one hand, spreading is not always the rule, as there are physical situations where the initial excitation does not vanish. This is the case of Anderson localization [3,4] or when the excitation remains topologically protected [5]. On the other hand, even in cases where the system seems to have reached an equilibrium state, the unitarity of quantum dynamics ensures a precise memory of the non-equilibrium initial condition. Then, if some experimental protocol could reverse the many-body dynamics, it would drive the system back to the initial non-equilibrium state [6]. Such a general idea defines the Loschmidt echo (LE), which embodies the various time-reversal procedures implemented in nuclear magnetic resonance (NMR) [7–9].

The first NMR time-reversal experiment was performed by Hahn in the 1950s [10]. The procedure, known as spin echo, reverses the precession dynamics of each independent spin around its local magnetic field by inverting the sign of the Zeeman energy. However, the sign of the energy associated with the spin–spin interactions is not inverted and, accordingly, the echo signal is degraded. Such a decay occurs within the time scale T_2 that characterizes the spin–spin interactions. Indeed, these interactions determine the survival of a spin excitation at short times as $\sim 1 - (t/T_2)^2$ and its later complex dynamics generating a diffusive spreading. By the early 1970s, Kessemeier, Rhim, Pines and Waugh implemented the reversal of the dynamics induced by the spin–spin dipolar interaction [11,12]. This results in the 'magic echo', which indicates the recovery of a global polarization state. Two decades later, Ernst and co-workers introduced the 'polarization echo' [13]. There, a local excitation injected in a many-spin system is allowed to evolve, then time-reversed and finally detected locally at the initial spot. While the success of these time-reversal echoes unambiguously evidenced the deterministic nature of spin dynamics in NMR, it is clear that the reversal is unavoidably degraded by uncontrolled internal or environmental degrees of freedom or by imperfections in the pulse sequences. Furthermore, the degradation seems to occur in a time scale, say T_3, much shorter than a naive estimation of the characteristic scale of these perturbations, say τ_Σ. Then, the question that arises is whether the complexity inherent to a large number of correlated spins would enhance the fragility of the procedure under perturbations.

The next generation of experiments in organic crystals [14–16] seemed to confirm that the experimental T_3 never exceeds a few times T_2. In other words, T_3 remains tied to the time scale that characterizes the reversible many-body interaction. This led to the postulate that, in an infinite many-spin system, the complex dynamics could favour the action of any small non-inverted interaction that perturbs the reversal procedure. Thus, reversible interactions become determinant for the irreversibility rate. This constitutes our *central hypothesis of irreversibility*. Such wisdom is further reinforced by the natural association of many-body complexity with a form of chaos [17,18] and the confirmation that quantum dynamics of classically chaotic systems should manifest a dynamical instability [19] which leads to an *environment-independent decoherence rate* [20,21].

During the last decade, solid-state NMR has kept on providing a versatile testing bench to study time reversal in large spin arrays [22–26]. In fact, a standard experiment involves a crystalline sample with an infinitely large number of spins. By contrast, the numerical test of many-spin dynamics has to be restricted to strictly finite systems [27,28]. While this appears to be a major limitation, it allows the analysis of a situation that the experiments cannot achieve: moving progressively from small systems to larger ones with a fully controlled perturbation. The expectation is that a sort of finite size scaling may allow one to identify an emergent mechanism that rules reversibility in the thermodynamic limit [29]. As in the experiments, the witness for such

a transition should be the LE as measured by a single spin autocorrelation function $M_{1,1}$, i.e. a local polarization. For short, we call $M_{1,1}$ the *local LE*. It is not difficult to prove that $\Pi_{1,1} \equiv (M_{1,1} + 1)/2$ is the probability that a given spin, say the first, remains up after the whole procedure. Besides, in a case of a spin excitation in a one-dimensional chain with *XY* interactions [30–32], $M_{1,1}$ precisely coincides [27] with the global overlap of two one-body wave functions as defined for semi-classical systems [20,33,34]. The square of the overlap between the initial and final many-body wave functions, M_{MB}, defines a *global* or *many-body LE*. It is important to note that M_{MB} has not been addressed experimentally, but nevertheless it is a natural magnitude in theory [35–37]. Thus, we are left without a precise relation between the object of theoretical studies and experimental ones, i.e. M_{MB} and $M_{1,1}$, respectively. This missing link is the central question we address in this paper.

Here, we consider a system of N spins whose initial state is given by a local excitation injected in a high-temperature state. First, we discuss the formal relation between M_{MB} and $M_{1,1}$, which is derived exactly at least for very short times. In particular, we assess how the N dependence or extensivity of M_{MB} is evidenced in the time scales involved. This leads us to hint that the revival of a many-spin state results from the recovery of each individual spin configuration, much as if they were statistically independent events. Because in the initial high-temperature state there are $N/2$ spins up, their rough statistical independence would lead to a behaviour of the sort $M_{MB} \sim (\Pi_{1,1})^{N/2} \sim (M_{1,1})^{N/4}$. This is confirmed by the numerical evaluation of the LE in a specific spin model.

Furthermore, we discuss a general picture beyond the short-time regime, where the decay of $M_{1,1}$ results from the interplay between the time scale that characterizes the reversible interactions (T_2) and that of the perturbation (τ_Σ). This would ultimately lead to the experimentally observed T_3. In such a sense, our analysis provides a conceptual link between the theoretical and the experimental realms.

The paper is organized as follows. In §2, we introduce the LE framework: the initial state and the time-reversal procedure. Here, we define both the local and global LEs. In §3, we compute the short-time expansions for the local LE and its non-local contributions (in particular, the many-body LE). This allows us to discuss a general picture of the LE decay in terms of the times scales that characterize M_{MB} and $M_{1,1}$. The dependence on N is discussed in terms of the extensivity of M_{MB} and statistical independence of the local autocorrelations. In §4, we assess our expectations by a numerical evaluation of the LE in a spin system. Section 5 summarizes our main conclusions and some of the important open questions in the field.

2. The Loschmidt echo in spin systems

Let us first specify the initial condition of a 'local excitation in a many-spin system'. We consider N spins $\frac{1}{2}$ in an infinite-temperature state, i.e. completely depolarized mixture, plus a locally injected polarization,

$$\hat{\rho}_0 = \frac{1}{2^N}(\hat{\mathbf{I}} + 2\hat{S}_1^z). \tag{2.1}$$

Here, the spin 1 is polarized while the others are not, i.e. $\text{tr}[\hat{S}_i^z \hat{\rho}_0] = \frac{1}{2}\delta_{i,1}$. Such an initial state can be experimentally implemented not only in NMR [38] but also in cold atoms [39].

As in the early LE experiments [14–16], our numerical evaluation focuses on an imperfect time-reversed evolution of the excitation, followed by a local measurement. The procedure is depicted in figure 1. A many-spin Hamiltonian $\hat{H}_0$ rules the *forward* evolution of the system up to a certain time t_R. At that moment, an inversion of the sign of $\hat{H}_0$ is performed, leading to a symmetric *backward* evolution. Nevertheless, there are unavoidable perturbations, denoted by $\hat{\Sigma}$, that could arise from the incomplete control of the Hamiltonian, acting on both periods. Thus, evolution operators for these t_R periods are $\hat{U}_+(t_R) = \exp[-(i/\hbar)(\hat{H}_0 + \hat{\Sigma})t_R]$ and $\hat{U}_-(t_R) = \exp[-(i/\hbar)(-\hat{H}_0 + \hat{\Sigma})t_R]$, respectively. It is quite practicable to define the LE operator as

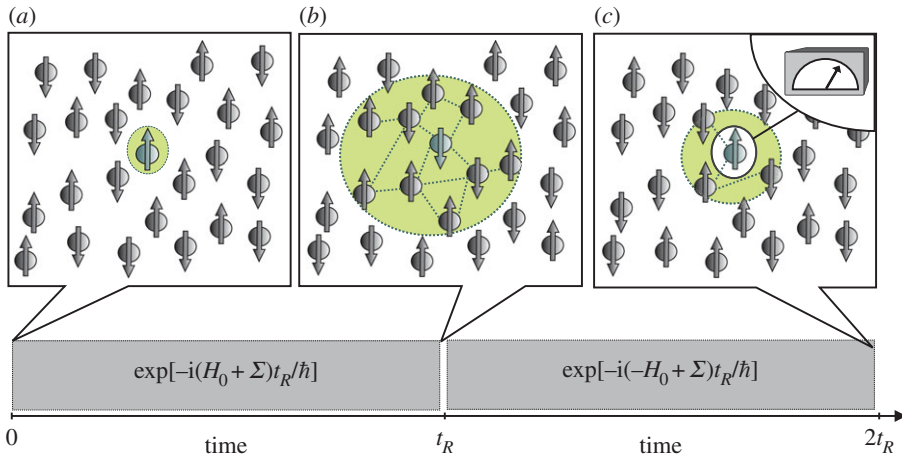$$\hat{U}_{LE}(2t_R) = \hat{U}_-(t_R)\hat{U}_+(t_R), \tag{2.2}$$

Figure 1. The scheme of the local LE, $M_{1,1}(t)$. (a) The initial state is given by a local excitation in a high-temperature spin system, as stated in equation (2.1). The system is allowed to evolve under the Hamiltonian $\hat{H}_0 + \hat{\Sigma}$ and the excitation diffuses all over until a time $t = t_R$ (b). At that time, a time reversal is performed, leading to a backward evolution ruled by $-\hat{H}_0 + \hat{\Sigma}$. At time $t = 2t_R$ (c), a local measurement is performed at the initial spot. (Online version in colour.)

which produces an imperfect refocusing at time $2t_R$. A local measurement of the polarization, performed at site 1, defines the local LE:

$$M_{1,1}(t) = 2\,\mathrm{tr}[\hat{S}_1^z \hat{U}_{\mathrm{LE}}(t)\hat{\rho}_0 \hat{U}_{\mathrm{LE}}^\dagger(t)] = 2\,\mathrm{tr}[\hat{S}_1^z \hat{\rho}_t]. \tag{2.3}$$

Here, we choose as free variable $t = 2t_R$, the total elapsed time in the presence of the perturbation. The time dependence of $\hat{\rho}_t$ in the Schrödinger picture is

$$\hat{\rho}_t = \hat{U}_{\mathrm{LE}}(t)\hat{\rho}_0 \hat{U}_{\mathrm{LE}}^\dagger(t). \tag{2.4}$$

Using equation (2.1), and after some algebraic manipulation, the LE can be explicitly written as a correlation function:

$$M_{1,1}(t) = \frac{1}{2^{N-2}}\,\mathrm{tr}[\hat{U}_{\mathrm{LE}}^\dagger(t)\hat{S}_1^z(0)\hat{U}_{\mathrm{LE}}(t)\hat{S}_1^z(0)] = \frac{\mathrm{tr}[\hat{S}_1^z(t)\hat{S}_1^z(0)]}{\mathrm{tr}[\hat{S}_1^z(0)\hat{S}_1^z(0)]}. \tag{2.5}$$

Here, the time dependence is written according to the Heisenberg picture,

$$\hat{S}_1^z(t) = \hat{U}_{\mathrm{LE}}^\dagger(t)\hat{S}_1^z(0)\hat{U}_{\mathrm{LE}}(t). \tag{2.6}$$

Note that equation (2.5) is an explicit correlation function at the same site but different times, i.e. an *auto*correlation. This kind of correlation has been recently employed to address localization phenomena in spin systems [4,40,41], and it generalizes the standard one employed to assess spin diffusion [42]. In terms of the Hilbert–Schmidt inner product between the initial and the time-evolved density matrices, i.e. equations (2.1) and (2.4) respectively, the LE can be written as [15,43,44]

$$M_{1,1}(t) = 2^N\,\mathrm{tr}[\hat{\rho}_0\hat{\rho}_t] - 1 = 2\frac{\mathrm{tr}[\hat{\rho}_0\hat{\rho}_t]}{\mathrm{tr}[\hat{\rho}_0\hat{\rho}_0]} - 1, \tag{2.7}$$

which, in the present case, progressively decays from 1 to 0, as occurs with the statistical overlap between two wave packets in the standard LE definition [20].

Equivalent expressions for the LE can be derived by decomposing the statistical state into a simpler basis. In order to proceed with the pure state decomposition of $\hat{\rho}_0$, we consider the computational Ising basis $\{|\beta_i\rangle\}$, also known as the S^z-decoupled basis. Additionally, we define the set $\mathcal{A}$ of indices j that label basis states which have the first spin pointing up, i.e. $j \in \mathcal{A} \Leftrightarrow$

$\hat{S}_1^z|\beta_j\rangle = +\frac{1}{2}|\beta_j\rangle$. It is straightforward to verify that $\hat{\rho}_0 = \sum_{j\in\mathcal{A}} 2^{-(N-1)}|\beta_j\rangle\langle\beta_j|$. Then, as introduced in [30],

$$M_{1,1}(t) = 2\left[\sum_{i\in\mathcal{A}}\sum_{j\in\mathcal{A}}\frac{1}{2^{N-1}}|\langle\beta_j|\hat{U}_{\mathrm{LE}}(t)|\beta_i\rangle|^2 - \frac{1}{2}\right] = 2\left[\Pi_{1,1}(t) - \frac{1}{2}\right]. \tag{2.8}$$

Here, $\Pi_{1,1}(t)$ denotes the *probability* that the first spin keeps pointing up after a time t. After some manipulation,

$$M_{1,1}(t) = 2\left[\sum_{i\in\mathcal{A}}\sum_{j\in\mathcal{A}}\frac{1}{2^{N-1}}|\langle\beta_j|\hat{U}_{\mathrm{LE}}(t)|\beta_i\rangle|^2 - \frac{1}{2}\right]$$

$$= \left[\sum_{i\in\mathcal{A}}\frac{1}{2^{N-1}}\left(|\langle\beta_i|\hat{U}_{\mathrm{LE}}(t)|\beta_i\rangle|^2 + \sum_{j\in\mathcal{A}\,(j\neq i)}|\langle\beta_j|\hat{U}_{\mathrm{LE}}(t)|\beta_i\rangle|^2 - \sum_{j\in\mathcal{B}}|\langle\beta_j|\hat{U}_{\mathrm{LE}}(t)|\beta_i\rangle|^2\right)\right]. \tag{2.9}$$

Here, $\mathcal{B}$ stands for the complement of $\mathcal{A}$, i.e. $j\in\mathcal{B} \Leftrightarrow \hat{S}_1^z|\beta_j\rangle = -\frac{1}{2}|\beta_j\rangle$. One can naturally identify and define the two terms that contribute to the local polarization $M_{1,1}(t)$. The first sum in equation (2.9) stands for the average probability of revival of the many-body states, denoted by $M_{\mathrm{MB}}(t)$,

$$M_{\mathrm{MB}}(t) = \sum_{i\in\mathcal{A}}\frac{1}{2^{N-1}}|\langle\beta_i|\hat{U}_{\mathrm{LE}}(t)|\beta_i\rangle|^2. \tag{2.10}$$

The second sum in equation (2.9) represents the average probability of changing the configuration of any spin except the first. The third sum stands for the average probability that the first spin has actually flipped, i.e. of all those processes that do not contribute to $M_{1,1}(t)$. Then, the processes that contribute to $M_{1,1}(t)$ but not to $M_{\mathrm{MB}}(t)$ are denoted as

$$M_X(t) = \sum_{i\in\mathcal{A}}\frac{1}{2^{N-1}}\left(\sum_{j\in\mathcal{A}\,(j\neq i)}|\langle\beta_j|\hat{U}_{\mathrm{LE}}(t)|\beta_i\rangle|^2 - \sum_{j\in\mathcal{B}}|\langle\beta_j|\hat{U}_{\mathrm{LE}}(t)|\beta_i\rangle|^2\right). \tag{2.11}$$

This balance of probabilities leads to the appropriate asymptotic behaviour of $M_{1,1}(t)$ according to the symmetries that constrain the evolution. The identification

$$M_{1,1}(t) = M_{\mathrm{MB}}(t) + M_X(t) \tag{2.12}$$

is a crucial step for the following discussions.

If we use the identity $\hat{S}_1^z = \hat{S}_1^+\hat{S}_1^- - \frac{1}{2}\hat{\mathbf{I}}$ in equation (2.5), the invariance of the trace under cyclic permutations ensures that $\mathrm{tr}[\hat{S}_1^z(t)\hat{S}_1^z(0)] = \mathrm{tr}[\hat{S}_1^-(0)\hat{S}_1^z(t)\hat{S}_1^+(0)] - \frac{1}{2}\mathrm{tr}[\hat{S}_1^z(t)]$. As $\mathrm{tr}[\hat{S}_1^z(t)] = \mathrm{tr}[\hat{S}_1^z(0)] = 0$, then

$$M_{1,1}(t) = 2\sum_i\frac{1}{2^{N-1}}\langle\beta_i|\hat{S}_1^-(0)\hat{U}_{\mathrm{LE}}^\dagger(t)\hat{S}_1^z(0)\hat{U}_{\mathrm{LE}}(t)\hat{S}_1^+(0)|\beta_i\rangle$$

$$= 2\sum_{i\in\mathcal{A}}\frac{1}{2^{N-1}}\langle\beta_i|\hat{U}_{\mathrm{LE}}^\dagger(t)\hat{S}_1^z\hat{U}_{\mathrm{LE}}(t)|\beta_i\rangle, \tag{2.13}$$

which is indeed an explicit way to rewrite equation (2.3) in the form of an ensemble average. Remarkably, as $\hat{S}_1^z$ is a local (one-body) operator, its evaluation in equation (2.13) can be replaced by the expectation value in a single superposition state [45],

$$M_{1,1}(t) = 2\langle\Psi_{\mathrm{neq}}|\hat{U}_{\mathrm{LE}}^\dagger(t)\hat{S}_1^z\hat{U}_{\mathrm{LE}}(t)|\Psi_{\mathrm{neq}}\rangle, \tag{2.14}$$

where

$$|\Psi_{\mathrm{neq}}\rangle = \sum_{i\in\mathcal{A}}\frac{1}{\sqrt{2^{N-1}}}\mathrm{e}^{\mathrm{i}\varphi_i}|\beta_i\rangle. \tag{2.15}$$

6

rsta.royalsocietypublishing.org *Phil. Trans. R. Soc. A* **374**: 20150163

Here, φ_i is a random phase uniformly distributed in $[0, 2\pi)$. In fact, the state defined in equation (2.15) is a random superposition that can successfully mimic the dynamics of ensemble calculations and provides a quadratic speed-up of computational efforts [45–47].

3. The Loschmidt echo dynamics

(a) Short-time expansions and beyond

In order to analyse the N dependence of the LE and its time scales, we compute here the short-time expansion of the magnitudes $M_{1,1}(t)$, $M_{\mathrm{MB}}(t)$ and $M_X(t)$. Up to second order in time,

$$M_{1,1}(t = 2t_R) = 2 \sum_{i \in \mathcal{A}} \frac{1}{2^{N-1}} \langle \beta_i | \hat{U}_{\mathrm{LE}}^{\dagger}(t) \hat{S}_1^z \hat{U}_{\mathrm{LE}}(t) | \beta_i \rangle$$

$$= 1 - \left(\frac{t}{\hbar} \right)^2 \sum_{i \in \mathcal{A}} \frac{1}{2^{N-1}} (\langle \beta_i | \hat{\Sigma}^2 | \beta_i \rangle - 2 \langle \beta_i | \hat{\Sigma} \hat{S}_1^z \hat{\Sigma} | \beta_i \rangle) + \mathcal{O}\left(\left(\frac{t}{\hbar} \right)^3 \right). \quad (3.1)$$

Similarly, the leading contributions to $M_{\mathrm{MB}}(t)$ and $M_X(t)$ are

$$M_{\mathrm{MB}}(t) = \sum_{i \in \mathcal{A}} \frac{1}{2^{N-1}} |\langle \beta_i | \hat{U}_{\mathrm{LE}}(t) | \beta_i \rangle|^2$$

$$= 1 - \left(\frac{t}{\hbar} \right)^2 \sum_{i \in \mathcal{A}} \frac{1}{2^{N-1}} (\langle \beta_i | \hat{\Sigma}^2 | \beta_i \rangle - \langle \beta_i | \hat{\Sigma} | \beta_i \rangle^2) + \mathcal{O}\left(\left(\frac{t}{\hbar} \right)^3 \right) \quad (3.2)$$

and

$$M_X(t) = \sum_{i \in \mathcal{A}} \frac{1}{2^{N-1}} \left(\sum_{j \in \mathcal{A}\,(j \neq i)} |\langle \beta_j | \hat{U}_{\mathrm{LE}}(t) | \beta_i \rangle|^2 - \sum_{j \in \mathcal{B}} |\langle \beta_j | \hat{U}_{\mathrm{LE}}(t) | \beta_i \rangle|^2 \right)$$

$$= \left(\frac{t}{\hbar} \right)^2 \sum_{i \in \mathcal{A}} \frac{1}{2^{N-1}} (2 \langle \beta_i | \hat{\Sigma} \hat{S}_1^z \hat{\Sigma} | \beta_i \rangle - \langle \beta_i | \hat{\Sigma} | \beta_i \rangle^2) + \mathcal{O}\left(\left(\frac{t}{\hbar} \right)^3 \right). \quad (3.3)$$

Let us consider a generic *secular* (i.e. polarization-conserving) perturbation $\hat{\Sigma}$ given by a Hamiltonian with an arbitrary anisotropy α,

$$\hat{\Sigma} = \sum_{i,j}^{N} (J_{\Sigma})_{ij} [2\alpha \hat{S}_i^z \hat{S}_j^z - (\hat{S}_i^x \hat{S}_j^x + \hat{S}_i^y \hat{S}_j^y)]. \quad (3.4)$$

This is still quite general, as even a double quantum perturbation ($\hat{S}_i^+ \hat{S}_j^+ + \hat{S}_i^- \hat{S}_j^-$, which does not conserve polarization) can be reduced to a secular one by the truncating effects of radiofrequency fields [29]. In addition, we do not consider here the case $[\hat{\Sigma}, \hat{S}_1^z] = 0$ (e.g. pure Ising or on-site diagonal disorder), as in such a condition the first non-trivial order in time is the fourth (see Appendix). Then, the following identities hold:

$$\sum_{i \in \mathcal{A}} \frac{1}{2^{N-1}} \langle \beta_i | \hat{\Sigma}^2 | \beta_i \rangle = 2N\sigma^2 \left(\frac{\alpha^2}{4} + \frac{1}{8} \right), \quad (3.5)$$

$$\sum_{i \in \mathcal{A}} \frac{1}{2^{N-1}} \langle \beta_i | \hat{\Sigma} \hat{S}_1^z \hat{\Sigma} | \beta_i \rangle = 2N\sigma^2 \left(\frac{\alpha^2}{8} + \frac{1}{16} \right) - \frac{1}{2}\sigma^2 \quad (3.6)$$

and

$$\sum_{i \in \mathcal{A}} \frac{1}{2^{N-1}} \langle \beta_i | \hat{\Sigma} | \beta_i \rangle^2 = 2N\sigma^2 \frac{\alpha^2}{4}. \quad (3.7)$$

Here, σ^2 stands for the average local second moment of $\hat{\Sigma}$,

$$\sigma^2 = \frac{1}{N} \sum_{i=1}^{N} \sigma_i^2 = \frac{1}{N} \sum_{i=1}^{N} \left[\sum_{j\,(\neq i)}^{N} \left(\frac{(J_\Sigma)_{ij}}{2} \right)^2 \right]. \tag{3.8}$$

Being a *perturbation*, we note that σ^2 is much smaller than the average local second moment σ_0^2 of the unperturbed Hamiltonian $\hat{H}_0$. In terms of time scales,

$$T_2 = \frac{\hbar}{\sqrt{\sigma_0^2}} \ll \frac{\hbar}{\sqrt{\sigma^2}} = \tau_\Sigma. \tag{3.9}$$

The identities in equations (3.5)–(3.7) lead to

$$M_{1,1}(t) = 1 - \left(\frac{t}{\tau_\Sigma} \right)^2 + \mathcal{O}\left(\left(\frac{t}{\hbar} \right)^3 \right), \tag{3.10}$$

$$M_{MB}(t) = 1 - \frac{1}{4} N \left(\frac{t}{\tau_\Sigma} \right)^2 + \mathcal{O}\left(\left(\frac{t}{\hbar} \right)^3 \right) \tag{3.11}$$

and

$$M_X(t) = \left(\frac{N-4}{4} \right) \left(\frac{t}{\tau_\Sigma} \right)^2 + \mathcal{O}\left(\left(\frac{t}{\hbar} \right)^3 \right). \tag{3.12}$$

These expansions hold for $t < (\tau_\Sigma/N)$. Beyond such a very short-time regime, a general term in the expansion of $M_{1,1}(t)$ will be of the form

$$\frac{c_{(N,n)} t^n}{(\tau_\Sigma^k T_2^{n-k})} \tag{3.13}$$

with $k \geq 2$ and the coefficient $c_{(N,n)}$ described by combinatorial numbers of increasing size that depend on the topology of the interactions (e.g. see [25,48]). As the experimental set-up corresponds to the limit described by equation (3.9), this expansion will be dominated by terms with the lowest possible order in the weak interaction, i.e. $k = 2$:

$$\left(\frac{t}{\tau_\Sigma} \right)^2 \left[1 + \sum_n c_{(N,n)} \left(\frac{t}{T_2} \right)^{n-2} \right]. \tag{3.14}$$

Equation (3.14) indicates that, beyond the very short-time expansion, i.e. $(\tau_\Sigma/N) < t < \tau_\Sigma$, the dependence on τ_Σ becomes superseded by the diverging terms in the scale T_2. This could lead to the new time scale T_3, which was seen experimentally to be tied to T_2 as

$$T_2 \lesssim T_3 \ll \tau_\Sigma. \tag{3.15}$$

In that sense, T_3 becomes characteristic of the complexity or 'chaos' of the many-spin system that amplifies the small effect of the perturbation. In addition, it is important to stress that, being an experimental fact, equation (3.15) corresponds to a system composed by infinitely many interacting spins. In other words, equation (3.15) stands for the relations of time scales in the thermodynamic limit. Quite on the contrary, any numerical simulation involves a finite, very small indeed, number of spins where the irreversibility rate T_3 would be essentially given by τ_Σ. Then, the LE decay rate evaluated in a finite system would ultimately be perturbation-dependent [28]. Thus, our *central hypothesis of irreversibility* would mean that equation (3.15) is an *emergent* property. It should rely on the thermodynamic limit, which implies taking the limit $N \to \infty$ first, and then $\tau_\Sigma \to \infty$. The non-uniformity of these limits plays a crucial role to yield quantum phase transitions, as discussed in the context of Anderson localization [49–51].

The physical picture described above is schematically represented in figure 2. There, we show the expected interplay between $M_{MB}(t)$ and $M_X(t)$ leading to $M_{1,1}(t)$. Indeed, as stated in equations (3.11) and (3.12), the very short-time dependence of both contributions is extensive in
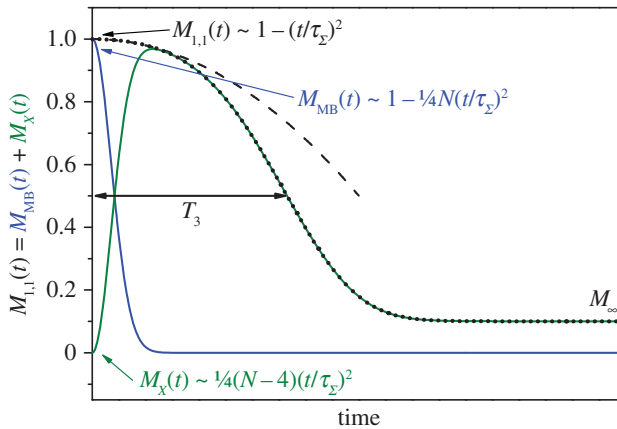
Figure 2. A pictorial scheme of the time dependence of $M_{1,1}(t)$ (black dotted line) and its contributions, as indicated by the labels, $M_{MB}(t)$ (blue solid line) and $M_X(t)$ (green solid line). Their short-time expansions, as stated in equations (3.10)–(3.12), are indicated with arrows. In particular, the expansion corresponding to the short-time behaviour of $M_{1,1}(t)$ is plotted with a black dashed line. (Online version in colour.)

N: $M_{MB}(t)$ decreases as $1 - N\sigma^2 t^2/4$ and $M_X(t)$ increases as $(N-4)\sigma^2 t^2/4$. Such a precise balance provides for the short-time decay of $M_{1,1}(t)$ given by equation (3.10), i.e. $1 - \sigma^2 t^2$. Note that there is no reason to assume that the decay of $M_{MB}(t)$ would remain ruled by τ_Σ. Beyond the very short times, we expect that the time scale T_3 should also show up as T_3/N^ν with $\nu \sim 1$ in the decay of $M_{MB}(t)$ (see below). Furthermore, while $M_{MB}(t)$ goes monotonically to zero, $M_X(t)$ displays a highly non-trivial behaviour. Indeed, $M_X(t)$ first increases by feeding from the decay of $M_{MB}(t)$ until it reaches a maximum. This growth indicates a progressive divergence of long-range correlations. Thereafter, $M_X(t)$ should decay, accounting for the fact that the state remains properly normalized. This is precisely what $M_{1,1}(t)$ measures: a conserved polarization that ultimately distributes uniformly within the spin system. In an isolated finite system this implies the asymptotic plateau $M_\infty \sim 1/N$. As pointed out above, the decay of both $M_{1,1}(t)$ and $M_X(t)$ occurs in a time scale T_3, which, according to equation (3.14), is somewhat longer than but close to the 'diffusion' time T_2. This is the regime captured experimentally.

(b) The extensive decay hypothesis

The previous short-time expansions provide a hint on the scaling relation between the local LE, $M_{1,1}(t)$, and the global one as embodied by $M_{MB}(t)$. In particular, let us first compare the probability of refocusing the configuration (up or down) of a single spin, i.e. $\Pi_{1,1}(t)$, and the probability of refocusing a complete many-spin state $M_{MB}(t)$. If the refocusing of each individual spin could be treated as an independent event, then the scaling between $\Pi_{1,1}$ and M_{MB} would be extensive in N,

$$(\Pi_{1,1}(t))^{N/2} \simeq M_{MB}(t). \tag{3.16}$$

Here, the factor $\frac{1}{2}$ in the exponent comes from equation (2.1), i.e. the initial high-temperature state, where basically half of the spins point up, and half of them point down. Then, one can resort to the picture of a lattice gas where $N/2$ particles jump among N lattice sites. As in the well-known Jordan–Wigner transformation [52], a fermion is associated with a spin pointing up and a vacancy corresponds to a spin pointing down. Thus, the microstate of the gas is completely described by the position of $N/2$ particles.

Strictly speaking, the notion of *extensiveness* corresponds to standard thermodynamic quantities such as the entropy of the system. In addition, as discussed in [16], $S = -\ln(M_{1,1}(t))$

is precisely a measure of the entropy. Then, the validity of equation (3.16) implies an extensivity relation between the entropy per spin and the total entropy of the system.

According to equations (2.8) and (3.10),

$$\Pi_{1,1}(t) = 1 - \frac{1}{2}\left(\frac{t}{\tau_\Sigma}\right)^2 + \mathcal{O}\left(\left(\frac{t}{\hbar}\right)^3\right), \tag{3.17}$$

which, in turn, up to second order in time, implies $\Pi_{1,1}(t) \simeq (M_{1,1}(t))^{1/2}$. Thus, equation (3.16) yields

$$(M_{1,1}(t))^{N/4} \simeq M_{\mathrm{MB}}(t). \tag{3.18}$$

This is precisely the relation verified between equations (3.10) and (3.11).

One might expect that, beyond the very short-time decay, individual spin autocorrelations deviate from statistical independence. However, this deviation will still have a local nature and, therefore, the N-extensivity would remain valid. Indeed, we propose

$$(M_{1,1}(t))^\eta \simeq M_{\mathrm{MB}}(t), \tag{3.19}$$

where the exponent η would be some appropriate function $\eta = \eta(N,t)$. Our 'extensive decay hypothesis' implies that η factorizes,

$$\eta(N,t) = N \times f(t), \tag{3.20}$$

where $f(t)$ stands for a function that encloses information of the correlations originated by the system dynamics. Additionally,

$$\lim_{t \to 0^+} f(t) = \tfrac{1}{4} \tag{3.21}$$

is required in order to recover equation (3.18), i.e. statistical independence.

4. A one-dimensional model

The physical picture described above is discussed here in the light of a specific model. In particular, we assess the validity of equations (3.18) and (3.20). We consider a one-dimensional spin chain with an anisotropic interaction described by

$$\hat{H}_0 = \sum_{i=1}^{N-1} J_0 \left(\frac{1}{2}\hat{S}_i^z \hat{S}_{i+1}^z + \hat{S}_i^x \hat{S}_{i+1}^x + \hat{S}_i^y \hat{S}_{i+1}^y\right) \tag{4.1}$$

with periodic boundary conditions, i.e. a ring configuration. Here, J_0 stands for the natural units of the spin–spin interaction energy. As a perturbation $\hat{\Sigma}$, we choose a next-nearest-neighbour interaction described by

$$\hat{\Sigma} = \sum_{i=1}^{N-2} J_\Sigma \left(\frac{1}{2}\hat{S}_i^z \hat{S}_{i+2}^z + \hat{S}_i^x \hat{S}_{i+2}^x + \hat{S}_i^y \hat{S}_{i+2}^y\right). \tag{4.2}$$

Such a perturbation appears naturally when one attempts to build an effective one-body dynamics from linear crystals with dipolar interactions [53]. This is also the case in a regular crystal, when the natural non-secular dipole–dipole terms are truncated by the Zeeman energy of the radiofrequency irradiation, which ultimately leads to effective secular two-body next-nearest-neighbour interactions [29].

The local second moments σ^2 and σ_0^2 of $\hat{\Sigma}$ and $\hat{H}_0$, respectively, can be evaluated as in equation (3.8) as

$$\sigma^2 = \tfrac{1}{2}(J_\Sigma)^2 \tag{4.3}$$

and

$$\sigma_0^2 = \tfrac{1}{2}(J_0)^2, \tag{4.4}$$

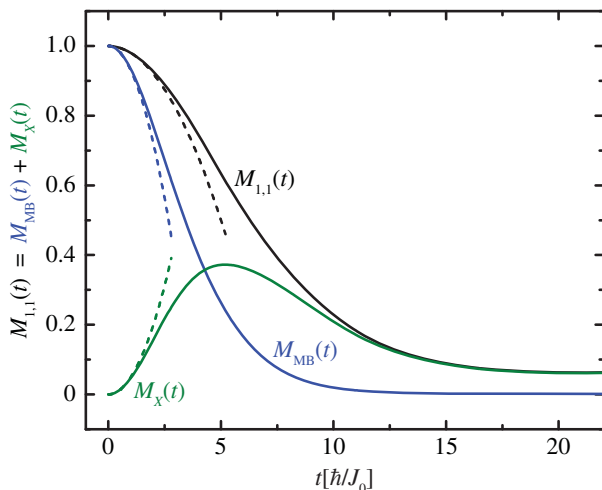and constitute the main energy scales of our problem.

Figure 3. The local LE and its non-local contributions. $M_{1,1}(t)$, $M_{MB}(t)$ and $M_X(t)$ correspond to the black, blue and green solid lines, as indicated by the labels; $N = 14$, $J_\Sigma = 0.1 J_0$. The short-time expansions given in equations (3.10)–(3.12) are shown as black, blue and green dashed lines, respectively. (Online version in colour.)
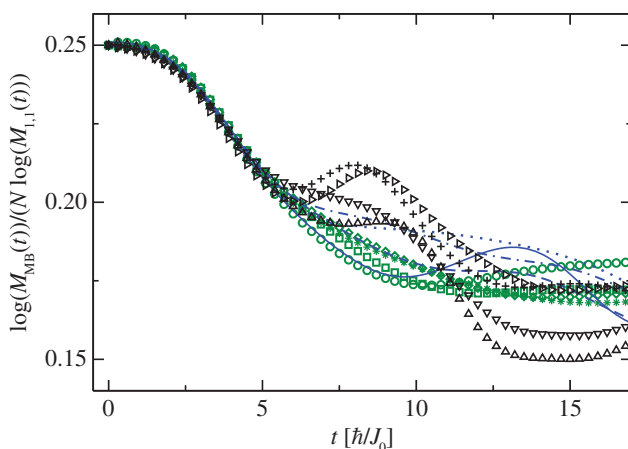

Figure 4. The relation $\log(M_{MB}(t))/(N \log(M_{1,1}(t)))$ as a function of time. For $J_\Sigma = 0.1 J_0$, the sizes plotted are: $N = 10$ (circles), $N = 12$ (squares), $N = 14$ (diamonds) and $N = 16$ (stars). For $J_\Sigma = 0.2 J_0$, the sizes plotted are: $N = 10$ (solid line), $N = 12$ (dashed line), $N = 14$ (dash-dotted line) and $N = 16$ (dotted line). For $J_\Sigma = 0.3 J_0$, the sizes plotted are: $N = 10$ (up triangles), $N = 12$ (down triangles), $N = 14$ (plus signs) and $N = 16$ (right triangles). (Online version in colour.)

In figure 3, we plot $M_{1,1}(t)$, $M_{MB}(t)$ and $M_X(t)$ for the particular choice $J_\Sigma = 0.1 J_0$. The short-time expansions given in equations (3.10)–(3.12) are evaluated according to equation (4.3). It is observed that $M_{MB}(t)$ vanishes for long times. Actually, a close observation shows that $M_{MB}(t \to \infty) \sim \mathcal{O}(2^{-N})$ (data not shown). In addition, note that $M_X(t \to \infty) \sim 1/N$. Such an asymptotic contribution provides for the equidistribution of the spin polarization $M_{1,1}(t \to \infty) \sim 1/N$. This long-time saturation corresponds to the equilibration of a finite system.

In contrast with our schematic plot in figure 2, here $M_X(t)$ does not get too close to 1 and $M_{MB}(t)$ does not decay much faster than $M_{1,1}(t)$. As $M_X(t)$ provides for the whole $M_{1,1}(t)$ once $M_{MB}(t)$ has fully decayed, the contribution of $M_X(t)$ is considerable only at long times. These effects are a consequence of the relatively small size of the system considered. Indeed, the case in figure 3 corresponds to $N = 14$ spins, and thus the exponent that relates $M_{1,1}(t)$ and $M_{MB}(t)$

is quite small, $(N/4) = 3.5$. The need for larger systems indicates that revealing the dominant orders in equation (3.14) is a major numerical challenge that may go beyond the state-of-the-art techniques [54].

In order to assess the accuracy of the 'extensive decay hypothesis', in figure 4, we address the scaling relation between $M_{1,1}(t)$ and $M_{MB}(t)$ discussed in §3b. In particular, we try out the factorization stated in equation (3.20). By plotting $\log(M_{MB}(t))/(\log(M_{1,1}(t))N)$ as a function of time, we observe a unique function which does not depend on N or J_Σ, but it has a weak dependence on time. Such a unique curve is indeed $f(t)$ as defined in equation (3.20). This means that the extensivity relation between $M_{1,1}(t)$ and $M_{MB}(t)$ is confirmed. The statistical independence, in turn, fails progressively once $f(t)$ departs from the $\frac{1}{4}$ factor of the ideal relation in equations (3.18) and (3.21). As beyond the short-time regime $f(t)$ decreases with time, we conclude that the recovery of a single spin is tied to the recovery of its neighbours. Thus, the spins are positively correlated and the revival probability of the complete N-spin state is enhanced. This argument is particularly relevant in one-dimensional systems.

After the onset of the saturation regime, where $M_{1,1} \sim 1/N$ and $M_{MB} \sim \mathcal{O}(2^{-N})$, the universal scaling naturally becomes noisy and the curves for different N and J_Σ separate from each other. As the decay is faster for larger perturbations, the appearance of such a spurious behaviour is observed to occur first for the largest value of J_Σ considered ($J_\Sigma = 0.3J_0$, plus signs and triangles).

5. Conclusion

We presented a detailed analysis of the LE in interacting spin systems. As in the NMR experiments, a local version of the LE, $M_{1,1}$, is defined as a single spin autocorrelation function. Simultaneously, we define a global LE, M_{MB}, as the average of the square of the overlap between many-body wave functions that evolved under perturbed Hamiltonians. While the former constitutes a specific experimental observable, the latter has only been assessed theoretically. Here, we showed the formal relation between both magnitudes, as far as their characteristic time scales and N dependence are concerned.

By analysing a short-time expansion of $M_{1,1}$ and M_{MB}, we derived a precise relation between their time scales. In this regime, the decay of $M_{1,1}$ is given by the average local second moment of the perturbation ($\hbar/\tau_\Sigma = \sqrt{\sigma^2}$), and the decay of M_{MB} by N times the local scale ($N\hbar/\tau_\Sigma$). This relation hints at a scaling law $M_{MB} \sim (M_{1,1})^{N/4}$ that accounts for the extensivity of M_{MB}. In such a case, the recovery of a many-spin state results from the recovery of each individual spin, much as if they were independent events. The numerical evaluation in a specific spin model shows that the exponent slightly diminishes with time, starting from the initial $N/4$. This means that the recovery of a single spin is positively correlated with the probability of recovery of its neighbours, and thus it improves the probability of the revival of the complete N-spin state. A precise control of these correlations may hint at experimental access to the global autocorrelation, i.e. M_{MB}, just by measuring a single spin (local) autocorrelation $M_{1,1}$. This would require an experimental protocol capable to encode a local excitation into a correlated many-spin state.

In addition, we discussed a general dynamical picture beyond the very short-time regime. There, the decay of $M_{1,1}$ results from the interplay between the time scale that characterizes the reversible interactions (T_2) and that of the perturbation (τ_Σ). This would ultimately lead to the experimentally observed T_3, which was found to be roughly independent of τ_Σ but closely related to T_2. The theoretical quest for the emergent T_3 time scale remains open and it may be beyond the reach of current numerical approaches. Assessing a fair estimate analytically would require a detailed account of the higher-order processes that dress the quadratic term in the perturbative expansion.

Note that our discussion led us to identify T_3, and hence the spin–spin interaction time T_2, as the time scales characterizing the complexity or many-spin chaos. As such, they show up not only in the decay of $M_{1,1}$ and M_{MB}, but also in the growth of $M_X = M_{1,1} - M_{MB}$. Indeed, in the field of anti-de Sitter/conformal field theory (AdS/CFT) correspondence there is an increasing interest in characterizing the role of chaos in quantum dynamics [55–58].

There, chaos manifests in the growth of four-body correlation functions, following an early suggestion by Larkin & Ovchinnikov [59]. They employed semiclassical arguments to address disordered superconductors and probed that the square dispersion of momentum should grow exponentially in a time scale determined by the collisions with impurities, i.e. with the unperturbed Hamiltonian (in our physical picture, T_2). Similarly, our average multi-spin correlation M_X would ultimately diverge within a time scale T_3/N, i.e. independent of the perturbation. This is indeed a measure of the decoherence, and hence of irreversibility, induced by many-spin chaos. Of course, we do not have a precise characterization of this time scale or the specific mathematical dependence on time. Thus, this is a puzzling issue to explore in the field of many-body chaos. Besides the obvious relevance for statistical mechanics and experimental physics, this might also contribute to a possible pathway between quantum mechanics and gravity.

Appendix A

It is worth mentioning that the very short-time expansions in equations (3.10)–(3.12) do not depend on the anisotropy α of the perturbation. In general, it can be proved that if $[\hat{\Sigma}, \hat{S}_1^z] = 0$ then

$$M_{1,1}(t) = 1 - \frac{(t/\hbar)^4}{2^{N+3}} \sum_{i \in \mathcal{A}} (2\langle \beta_i | [\hat{\Sigma}, \hat{H}_0] \hat{S}_1^z [\hat{\Sigma}, \hat{H}_0] | \beta_i \rangle - \langle \beta_i | [\hat{\Sigma}, \hat{H}_0]^2 | \beta_i \rangle) + \mathcal{O}\left(\left(\frac{t}{\hbar}\right)^5\right). \quad (A\,1)$$

This is precisely the case of a perturbation $\hat{\Sigma}$ enclosing Anderson disorder and Ising interactions [40] or interactions with a fluctuating field [60].

References

1. Blume M, Hubbard J. 1970 Spin correlation functions at high temperatures. *Phys. Rev. B* **1**, 3815–3830. (doi:10.1103/PhysRevB.1.3815)
2. Forster D. 1975 *Hydrodynamic fluctuations, broken symmetry, and correlation functions*. Frontiers in Physics, vol. 47. Reading, MA: WA Benjamin.
3. Basko DM, Aleiner IL, Altshuler BL. 2006 Metal insulator transition in a weakly interacting many-electron system with localized single-particle states. *Ann. Phys.* **321**, 1126–1205. (doi:10.1016/j.aop.2005.11.014)
4. Zangara PR, Levstein PR, Pastawski HM. 2015 Role of energy uncertainties in ergodicity breaking induced by competing interactions and disorder. A dynamical assessment through the Loschmidt echo. *Pap. Phys.* **7**, 070012. (doi:10.4279/PIP.070012)
5. Wen XG. 2004 *Quantum field theory of many-body systems from the origin of sound to an origin of light and electrons*. New York, NY: Oxford University Press.
6. Brewer RG, Hahn EL. 1984 Atomic memory. *Sci. Am.* **251**, 50–57. (doi:10.1038/scientific american1284-50)
7. Gorin T, Prosen T, Seligman TH, Znidaric M. 2006 Dynamics of Loschmidt echoes and fidelity decay. *Phys. Rep.* **435**, 33–156. (doi:10.1016/j.physrep.2006.09.003)

13

8. Jacquod P, Petitjean C. 2009 Decoherence, entanglement and irreversibility in quantum dynamical systems with few degrees of freedom. *Adv. Phys.* **58**, 67–196. (doi:10.1080/00018730902831009)

9. Goussev A, Jalabert R, Pastawski H, Wisniacki D. 2012 Loschmidt echo. *Scholarpedia* **7**, 11687. (doi:10.4249/scholarpedia.11687)

10. Hahn EL. 1950 Spin echoes. *Phys. Rev.* **80**, 580–594. (doi:10.1103/PhysRev.80.580)

11. Rhim WK, Kessemeier H. 1971 Transverse-magnetization recovery in the rotating frame. *Phys. Rev. B* **3**, 3655–3661. (doi:10.1103/PhysRevB.3.3655)

12. Rhim WK, Pines A, Waugh JS. 1971 Time-reversal experiments in dipolar-coupled spin systems. *Phys. Rev. B* **3**, 684–696. (doi:10.1103/PhysRevB.3.684)

13. Zhang S, Meier BH, Ernst RR. 1992 Polarization echoes in NMR. *Phys. Rev. Lett.* **69**, 2149–2151. (doi:10.1103/PhysRevLett.69.2149)

14. Levstein PR, Usaj G, Pastawski HM. 1998 Attenuation of polarization echoes in nuclear magnetic resonance: a study of the emergence of dynamical irreversibility in many-body quantum systems. *J. Chem. Phys.* **108**, 2718–2724. (doi:10.1063/1.475664)

15. Pastawski HM, Levstein PR, Usaj G, Raya J, Hirschinger J. 2000 A nuclear magnetic resonance answer to the Boltzmann–Loschmidt controversy? *Physica A* **283**, 166–170. (doi:10.1016/S0378-4371(00)00146-1)

16. Usaj G, Pastawski HM, Levstein PR. 1998 Gaussian to exponential crossover in the attenuation of polarization echoes in NMR. *Mol. Phys.* **95**, 1229–1236. (doi:10.1080/00268979809483253)

17. Flambaum VV, Izrailev FM. 2000 Excited eigenstates and strength functions for isolated systems of interacting particles. *Phys. Rev. E* **61**, 2539–2542. (doi:10.1103/PhysRevE.61.2539)

18. Flambaum VV, Izrailev FM. 2001 Entropy production and wave packet dynamics in the Fock space of closed chaotic many-body systems. *Phys. Rev. E* **64**, 036220. (doi:10.1103/PhysRevE.64.036220)

19. Peres A. 1984 Stability of quantum motion in chaotic and regular systems. *Phys. Rev. A* **30**, 1610–1615. (doi:10.1103/PhysRevA.30.1610)

20. Jalabert RA, Pastawski HM. 2001 Environment-independent decoherence rate in classically chaotic systems. *Phys. Rev. Lett.* **86**, 2490–2493. (doi:10.1103/PhysRevLett.86.2490)

21. Cucchietti FM, Pastawski HM, Jalabert RA. 2004 Universality of the Lyapunov regime for the Loschmidt echo. *Phys. Rev. B* **70**, 035311. (doi:10.1103/PhysRevB.70.035311)

22. Krojanski HG, Suter D. 2004 Scaling of decoherence in wide NMR quantum registers. *Phys. Rev. Lett.* **93**, 090501. (doi:10.1103/PhysRevLett.93.090501)

23. Morgan SW, Oganesyan V, Boutis GS. 2012 Multispin correlations and pseudothermalization of the transient density matrix in solid-state NMR: free induction decay and magic echo. *Phys. Rev. B* **86**, 214410. (doi:10.1103/PhysRevB.86.214410)

24. Kaur G, Ajoy A, Cappellaro P. 2013 Decay of spin coherences in one-dimensional spin systems. *New J. Phys.* **15**, 093035. (doi:10.1088/1367-2630/15/9/093035)

25. Sánchez CM, Acosta RH, Levstein PR, Pastawski HM, Chattah AK. 2014 Clustering and decoherence of correlated spins under double quantum dynamics. *Phys. Rev. A* **90**, 042122. (doi:10.1103/PhysRevA.90.042122)

26. Álvarez GA, Suter D, Kaiser R. 2015 Localization–delocalization transition in the dynamics of dipolar-coupled nuclear spins. *Science* **349**, 846–848. (doi:10.1126/science.1261160)

27. Zangara PR, Dente AD, Levstein PR, Pastawski HM. 2012 Loschmidt echo as a robust decoherence quantifier for many-body systems. *Phys. Rev. A* **86**, 012322. (doi:10.1103/PhysRevA.86.012322)

28. Fine BV, Elsayed TA, Kropf CM, de Wijn AS. 2014 Absence of exponential sensitivity to small perturbations in nonintegrable systems of spins $\frac{1}{2}$. *Phys. Rev. E* **89**, 012923. (doi:10.1103/PhysRevE.89.012923)

29. Zangara PR, Bendersky D, Pastawski HM. 2015 Proliferation of effective interactions: decoherence-induced equilibration in a closed many-body system. *Phys. Rev. A* **91**, 042112. (doi:10.1103/PhysRevA.91.042112)

30. Pastawski HM, Levstein PR, Usaj G. 1995 Quantum dynamical echoes in the spin diffusion in mesoscopic systems. *Phys. Rev. Lett.* **75**, 4310–4313. (doi:10.1103/PhysRevLett.75.4310)

31. Pastawski HM, Usaj G, Levstein PR. 1996 Quantum interference phenomena in the local polarization dynamics of mesoscopic systems: an NMR observation. *Chem. Phys. Lett.* **261**, 329–334. (doi:10.1016/0009-2614(96)00978-5)

32. Mádi ZL, Brutscher B, Schulte-Herbrüggen T, Brüschweiler R, Ernst RR. 1997 Time-resolved observation of spin waves in a linear chain of nuclear spins. *Chem. Phys. Lett.* **268**, 300–305. (doi:10.1016/S0009-2614(97)00194-2)

33. Jacquod P, Silvestrov P, Beenakker C. 2001 Golden rule decay versus Lyapunov decay of the quantum Loschmidt echo. *Phys. Rev. E* **64**, 055203. (doi:10.1103/PhysRevE.64.055203)

34. Jacquod P, Adagideli I, Beenakker CWJ. 2002 Decay of the Loschmidt echo for quantum states with sub-Planck-scale structures. *Phys. Rev. Lett.* **89**, 154103. (doi:10.1103/PhysRevLett.89.154103)

35. Prosen T. 2007 Chaos and complexity of quantum motion. *J. Phys. A Math. Theor.* **40**, 7881–7918. (doi:10.1088/1751-8113/40/28/S02)

36. Torres-Herrera EJ, Vyas M, Santos LF. 2014 General features of the relaxation dynamics of interacting quantum systems. *New J. Phys.* **16**, 063010. (doi:10.1088/1367-2630/16/6/063010)

37. Torres-Herrera EJ, Santos LF. 2014 Quench dynamics of isolated many-body quantum systems. *Phys. Rev. A* **89**, 043620. (doi:10.1103/PhysRevA.89.043620)

38. Cappellaro P. 2014 Implementation of state transfer Hamiltonians in spin chains with magnetic resonance techniques. In *Quantum state transfer and network engineering* (eds GM Nikolopoulos, I Jex), pp. 183–222. Berlin, Germany: Springer.

39. Fukuhara T *et al.* 2013 Quantum dynamics of a mobile spin impurity. *Nat. Phys.* **9**, 235–241. (doi:10.1038/nphys2561)

40. Zangara PR, Dente AD, Iucci A, Levstein PR, Pastawski HM. 2013 Interaction–disorder competition in a spin system evaluated through the Loschmidt echo. *Phys. Rev. B* **88**, 195106. (doi:10.1103/PhysRevB.88.195106)

41. Serbyn M, Knap M, Gopalakrishnan S, Papić Z, Yao NY, Laumann CR, Abanin DA, Lukin MD, Demler EA. 2014 Interferometric probes of many-body localization. *Phys. Rev. Lett.* **113**, 147204. (doi:10.1103/PhysRevLett.113.147204)

42. Levstein PR, Pastawski HM, Calvo R. 1991 Spin diffusion in low-dimensional copper–amino-acid complexes. *J. Phys. Condens. Matter* **3**, 1877–1888. (doi:10.1088/0953-8984/3/12/018)

43. Cucchietti FM, Dalvit DAR, Paz JP, Zurek WH. 2003 Decoherence and the Loschmidt echo. *Phys. Rev. Lett.* **91**, 210403. (doi:10.1103/PhysRevLett.91.210403)

44. Bendersky D, Zangara PR, Pastawski HM. 2013 Fragility of superposition states evaluated by the Loschmidt echo. *Phys. Rev. A* **88**, 032102. (doi:10.1103/PhysRevA.88.032102)

45. Álvarez GA, Danieli EP, Levstein PR, Pastawski HM. 2008 Quantum parallelism as a tool for ensemble spin dynamics calculations. *Phys. Rev. Lett.* **101**, 120503. (doi:10.1103/PhysRevLett.101.120503)

46. Elsayed TA, Fine BV. 2013 Regression relation for pure quantum states and its implications for efficient computing. *Phys. Rev. Lett.* **110**, 070404. (doi:10.1103/PhysRevLett.110.070404)

47. Pineda C, Prosen T, Villaseñor EV. 2014 Two dimensional kicked quantum Ising model: dynamical phase transitions. *New J. Phys.* **16**, 123044. (doi:10.1088/1367-2630/16/12/123044)

48. Domínguez FD, González CE, Segnorile HH, Zamar RC. 2016 Irreversible adiabatic decoherence of dipole-interacting nuclear-spin pairs coupled with a phonon bath. *Phys. Rev. A* **93**, 022120. (doi:10.1103/PhysRevA.93.022120)

49. Anderson PW. 1978 Local moments and localized states. *Rev. Mod. Phys.* **50**, 191–201. (doi:10.1103/RevModPhys.50.191)

50. Rodrigues DE, Pastawski HM, Weisz JF. 1986 Localization and phase coherence length in the Lloyd model. *Phys. Rev. B* **34**, 8545–8549. (doi:10.1103/PhysRevB.34.8545)

51. Pastawski HM. 2007 Revisiting the Fermi golden rule: quantum dynamical phase transition as a paradigm shift. *Physica B* **398**, 278–286. (doi:10.1016/j.physb.2007.05.024)

52. Lieb E, Schultz T, Mattis D. 1961 Two soluble models of an antiferromagnetic chain. *Ann. Phys.* **16**, 407–466. (doi:10.1016/0003-4916(61)90115-4)

53. Rufeil-Fiori E, Sánchez CM, Oliva FY, Pastawski HM, Levstein PR. 2009 Effective one-body dynamics in multiple-quantum NMR experiments. *Phys. Rev. A* **79**, 032324. (doi:10.1103/PhysRevA.79.032324)

54. Dente AD, Bederián CS, Zangara PR, Pastawski HM. 2013 GPU accelerated Trotter–Suzuki solver for quantum spin dynamics. (http://arxiv.org/abs/1305.0036)

55. Shenker SH, Stanford D. 2014 Black holes and the butterfly effect. *J. High Energy Phys.* **2014**(3), 67. (doi:10.1007/JHEP03(2014)067)

56. Sekino Y, Susskind L. 2008 Fast scramblers. *J. High Energy Phys.* **2008**(10), 065. (doi:10.1088/1126-6708/2008/10/065)
57. Roberts DA, Stanford D, Susskind L. 2015 Localized shocks. *J. High Energy Phys.* **2015**(3), 51. (doi:10.1007/JHEP03(2015)051)
58. Kitaev A. 2014 Hidden correlations in the Hawking radiation and thermal noise. Speech given at Fundamental Physics Prize Symp., Nov. 10, Stanford SITP seminars, Nov. 11 and Dec. 18.
59. Larkin AI, Ovchinnikov YN. 1969 Quasiclassical method in the theory of superconductivity. *J. Exp. Theor. Phys.* **28**, 1200.
60. Fernández-Alcázar LJ, Pastawski HM. 2015 Decoherent time-dependent transport beyond the Landauer–Büttiker formulation: a quantum-drift alternative to quantum jumps. *Phys. Rev. A* **91**, 022117. (doi:10.1103/PhysRevA.91.022117)

15

rsta.royalsocietypublishing.org *Phil. Trans. R. Soc. A* **374**: 20150163